Second Virial Coefficient Calculations for Square-Well Chain Molecules

John M. Wichert and Carol K. Hall*

Department of Chemical Engineering, North Carolina State University, Raleigh, North Carolina 27695-7905

Received September 27, 1993; Revised Manuscript Received February 24, 1994®

ABSTRACT: The second virial coefficient, B_2, has been calculated for square-well chain molecules of lengths n = 2–50 and well widths of λ = 0.25–1.0 by Monte Carlo integration. The theta temperature, at which B_2 = 0, is independent of chain length around λ = 0.5, increases with chain length for $\lambda > 0.5$, and decreases with chain length for $\lambda < 0.5$. A scaling relation, $T_\theta^*(n) - T_\theta^*(\infty) \propto n^{-\phi}$, accurately describes the departure of the theta temperature from the infinite chain length value for $\lambda \geq 0.6$. A closed-form expression for the second virial coefficient of square-well chains is presented which accurately fits the Monte Carlo data for n = 2–50 and λ = 0.25–0.75. When compared to the Monte Carlo results, the second virial coefficient predicted by the generalized Flory–dimer theory for square-well chains is found to be increasingly inaccurate as chain length increases. If we correct the generalized Flory–dimer equation of state by forcing it to have the correct second virial coefficient, the compressibility factor is accurately predicted at densities below η = 0.04.

1. Introduction

The development of molecularly based equations of state for polymer and hydrocarbon fluids has been of theoretical and practical interest over the past 50 years. One route to such an equation of state is the virial expansion, proposed in 1885 by Thiesen[1] and later developed by Kamerlingh Onnes.[2] The virial equation of state is an expansion of the pressure in powers of density; the coefficients in this expansion are called virial coefficients and depend only on the temperature. The virial expansion was essentially an empirical expression until it was put on more solid theoretical footing by Mayer[3] in the late 1930s. He derived exact expressions for the virial coefficients in terms of multibody interactions and found that the second virial coefficient depends explicitly on two-body interactions, the third virial coefficient depends on three-body interactions, and so on. Since it is an expansion in powers of the density, a truncated virial equation is most accurate at low densities.

An alternate approach to the development of molecularly based equations of state for polymer and hydrocarbon fluids is the mean-field approach. Over the past several years our group has adopted this approach in an effort to develop an equation of state for fluids containing chainlike molecules modeled either as freely jointed chains of tangent hard spheres[4,5] or as freely jointed chains of square-well spheres.[6] Equations of state for hard-chain fluids and square-well chain fluids have been obtained using the generalized Flory–dimer (GF-D) formalism, in which the properties of the chain fluid are related to the properties of fluids composed of monomers and dimers. Comparison of the resulting compressibility factors with computer simulation results shows good agreement at low density and excellent agreement at high densities. The discrepancy between the low- and high-density performances of the GF-D theory is not surprising since the mean-field arguments used in its derivation work best at high densities.

In this paper we use Monte Carlo integration to calculate the second virial coefficient for square-well chain fluids. This study is motivated partly by our desire to test and improve the low-density performance of the GF-D theory for square-well chain fluids and partly by our interest in studying the scaling behavior of the second virial coefficient for chain fluids. For the square-well chain model, each molecule is a chain of n tangent spheres of diameter σ that interact via a site–site square-well potential $u(r_{ij})$ which is given by $u(r_{ij}) = \infty$ for $r_{ij} \leq \sigma$, $u(r_{ij}) = -\epsilon$ for $\sigma < r_{ij} < (1 + \lambda)\sigma$, and $u(r_{ij}) = 0$ for $r_{ij} \geq (1 + \lambda)\sigma$, where r_{ij} is the distance between two sites i and j which are on different molecules. Sites on the same chain interact via hard-core repulsions only, for which $u(r_{ij}) = \infty$ for $r_{ij} \leq \sigma$ and $u(r_{ij}) = 0$ for $r_{ij} > \sigma$. The second virial coefficients are calculated for chains of length n = 2, 3, 4, 8, 16, 24, and 50 at well widths of λ = 0.25, 0.3, 0.4, 0.5, 0.6, 0.7, 0.75, and 1.0. Although the combination of a hard-core potential for intramolecular interactions and a square-well potential for intermolecular interactions is somewhat artificial in that it is equivalent to immersing a polymer molecule simultaneously in two different solvents, the behavior of this model is of interest because it is the same as the model used in the GF-D theory for square-well chains. It also has the advantage that extrapolation of the Monte Carlo results to different temperatures is straightforward. To model solvent conditions more realistically, we also consider the square-well site–site potential for both intermolecular and intramolecular interactions; from this we can gauge the effect of omitting intramolecular attractive potentials.

Before summarizing our results, it is useful to review previous calculations by Yethiraj et al.[7] for the second virial coefficient of hard chains, since our molecular model reduces to this case in the limit as $\lambda \to 0$ or as $T \to \infty$. Yethiraj et al. modeled athermal chains as a pearl necklace of freely jointed tangent hard spheres. The second virial coefficient was calculated for chains of length 2–128 by Monte Carlo integration. They found that the continuous-space second virial coefficients are higher than the corresponding values for lattice chains but lower than second virial coefficients predicted by the equation of state derived from GF-D theory.[6] Yethiraj et al. also proposed a modification to the GF-D equation of state to more accurately predict the compressibility factor at low density. Their corrected compressibility factor is

$$Z = Z_{\text{GF-D}} + (B_{2,\text{MC}} - B_{2,\text{GF-D}})\rho \qquad (1)$$

where Z is the compressibility factor, MC stands for Monte Carlo, and ρ is the number of molecules per unit volume.

® Abstract published in *Advance ACS Abstracts*, April 1, 1994.

0024-9297/94/2227-2744$04.50/0

The modified equation of state predicts compressibility factors more accurately than the uncorrected GF-D equation of state at low density ($\eta < 0.2$) for both 8-mers and 20-mers but is less accurate at high density ($\eta > 0.3$) for 8-mers (η (the volume fraction) = $n\rho\sigma^3/6$). They also derived a closed-form expression for the second virial coefficient of hard chains,

$$B_2 = \frac{n^2}{(1.240\sqrt{n-1} - 1.408)^{1/2}} \tag{2}$$

This equation has the correct scaling behavior for large n and is accurate in comparison with computer simulations to within 0.5% for $12 \leq n \leq 128$.

In this paper, we present a simple, closed-form expression for the second virial coefficient of square-well chains as a function of well width and chain length. Our expression has the form

$$B_2(n,\lambda,\beta) = B_2^{hc}(n) - C_1(n,\lambda)\left[\frac{e^{\beta\epsilon}}{1 - c(n,\lambda)e^{\beta\epsilon}} - \frac{1}{1 - c(n,\lambda)}\right] \tag{3}$$

where $\beta = 1/kT$, n is the chain length, λ is the well width, $B_2^{hc}(n)$ is the hard-chain second virial coefficient, $C_1(n,\lambda)$ is a function of site–site interchain attractions which is determined by Monte Carlo integration, and $c(n,\lambda)$ is an adjustable parameter. For $B_2^{hc}(n)$ we use eq 2, or a scaling relation. $C_1(n,\lambda)$ is accurately fit by

$$C_1(n,\lambda) = (0.1527 + 2.973\lambda)n^2(n-1)^{(-0.6841-0.3618\lambda)} \tag{4}$$

and $c(n,\lambda)$ is determined once we know the theta temperature. Equation 3 accurately fits the second virial coefficient data above the theta temperature for chains of length $2 \leq n \leq 24$ for the range of well widths $\lambda = 0.25$–0.75.

This paper also describes an investigation of the scaling behavior of the theta temperature for square-well chains. The theta temperature, $T_\theta(n)$, is the temperature at which the attractive and repulsive contributions to the second virial coefficient cancel. As chain length increases, the theta temperature approaches its infinite chain length value. The dependence of the theta temperature on chain length can be described by the scaling relation $T_\theta^*(n) - T_\theta^*(\infty) \propto n^{-\phi}$. This relation was also found to work well for lattice chains by Dickman.[12] Here we use the scaling relation to predict the infinite chain length theta temperature for square-well chains with well widths of $\lambda =$ 0.6, 0.7, 0.75, and 1.0. We have found that the theta temperature for square-well chains with $\lambda \leq 0.4$ decreases as chain length increases; for square-well chains with $\lambda \geq$ 0.6, the theta temperature increases as chain length increases. In comparison, other workers have found that for linear chains on a lattice, the theta temperature decreases as chain length increases.

The low-density behavior of the GF-D equation of state for square-well chains is investigated by comparing second virial coefficients predicted by the theory to our Monte Carlo calculations and comparing the compressibility factor predicted by the GF-D theory at low density to compressibility factors calculated by Monte Carlo simulation for square-well 8-mers and 20-mers. For all of the well widths studied, the GF-D theory is found to be an increasingly unreliable predictor of the second virial coefficient as chain length is increased. The closed-form expression presented here gives an accurate estimate of the second virial coefficient, especially above the theta temperature. The compressibility factor predicted by the GF-D equation of state for square-well chains is more accurate compared to simulations when the second virial correction, eq 1, is used, but the corrected equation is inaccurate above $\eta = 0.04$. The truncated virial expansion

$$Z = 1 + B_2\rho \tag{5}$$

is more accurate than the uncorrected GF-D equation of state but somewhat less accurate than the corrected GF-D equation of state at $\eta < 0.04$. Like the corrected GF-D equation of state for square-well chains, the truncated virial expansion fails above $\eta = 0.04$.

The rest of the paper is organized as follows: in section 2 the Monte Carlo method is presented. In section 3 the results of our second virial coefficient calculations for square-well chains are described, along with an analysis of the scaling behavior of the theta temperature. Also, a compact functional form for the second virial coefficient of square-well chains is presented. In section 4 the values of the second virial coefficient predicted by the GF-D equation of state are compared to our Monte Carlo calculations, and the second virial coefficients are used as a low-density correction to the GF-D equation of state. In section 5 the effect of intramolecular attractions on the theta temperature is investigated. Finally, in section 6 our results are summarized.

2. Monte Carlo Calculation of the Second Virial Coefficient

The second virial coefficient for a square-well chain fluid can be evaluated by Monte Carlo integration of the integral expression[13]

$$B_2 = -\frac{1}{2}\int F_1(\omega_1)\, F_2(\omega_2)\, f_{12}(\boldsymbol{r},\omega_1,\omega_2)\, d\boldsymbol{r}\, d\omega_1\, d\omega_2 \tag{6}$$

Here $\boldsymbol{r}$ is the vector between the centers of mass of chains 1 and 2, $F_1(\omega_1)$ and $F_2(\omega_2)$ are the distribution functions for the internal coordinates, ω_1 and ω_2, of chains 1 and 2,

$$F_1(\omega_1) = \frac{\exp[-\beta u_1(\omega_1)]}{Z_1(\omega_1)} \tag{7}$$

$$F_2(\omega_2) = \frac{\exp[-\beta u_2(\omega_2)]}{Z_2(\omega_2)} \tag{8}$$

$Z_1(\omega_1)$ and $Z_2(\omega_2)$ are the configurational partition functions, u_1 and u_2 are the intramolecular potentials of chains 1 and 2, and f_{12} is the Mayer f-function

$$f_{12}(\boldsymbol{r},\omega_1,\omega_2) = \exp(-\beta u(1,2)) - 1 \tag{9}$$

where $u(1,2)$ is the sum of the pair potentials between sites on chains 1 and 2. The integrand in eq 6 is negative if the interchain interaction is repulsive and positive if the interchain interaction is attractive. For hard chains, integrating eq 6 over all intramolecular configurations and intermolecular separations gives one-half the volume excluded by one chain to another chain.

For square-well chains, we evaluate eq 6 using method B of Yethiraj et al.[7] In this method, two chains are placed independently in a cubic box with periodic boundary conditions. The chains are then moved about the box by the "translation–jiggling" move of Dickman and Hall.[14] If we accept chain moves according to the Metropolis algorithm,[9] intramolecular configurations are sampled in

Table 1. Comparison of the Coefficients C_k in Eq 12 for Square-Well Dimers ($\lambda = 0.5$) Calculated in This Work to Those Calculated by Yethiraj et al.[10]

coefficient	this work	Yethiraj et al.
C_1	6.489(9)[a]	6.485
C_2	2.22(2)	2.22
C_3	0.523(4)	0.526
C_4	0.0827(11)	0.0829

[a] The numbers in parentheses are the 95% confidence limits.

proportion to their distribution function weights, $F_1(\omega_2)$ and $F_2(\omega_2)$, and eq 6 can be written

$$B_2 = -\frac{1}{2}\int f_{12}(\boldsymbol{r},\omega_1,\omega_2)\, d\boldsymbol{r}\, d\omega_1\, d\omega_2 \tag{10}$$

After every ten Monte Carlo moves, the f-function for the chains is calculated by checking interchain attractive and repulsive overlaps. In essence, the calculation of the attractive potential's contribution to the second virial coefficient boils down to evaluating the number of single, double, triple, quadruple, etc. attractive overlaps. This is because the second virial coefficient for square-well chains is identically equal to

$$B_2 = -\frac{1}{2}V_{box}\langle f_{12}\rangle_{r,\omega_1,\omega_2} = -\frac{1}{2}V_{box}\left[\frac{N_o}{N_p} + \frac{N_a^{(1)}}{N_p}(e^{\beta\epsilon}-1) + \frac{N_a^{(2)}}{N_p}(e^{2\beta\epsilon}-1) + \frac{N_a^{(3)}}{N_p}(e^{3\beta\epsilon}-1) + \ldots + \frac{N_a^{(m)}}{N_p}(e^{m\beta\epsilon}-1)\right] \tag{11}$$

where N_o is the number of hard-core overlaps, $N_a^{(k)}$ is the number of configurations which have k attractive overlaps and no repulsive overlaps, N_p is the total number of configurations checked for overlap, and $m \le n^2$ is the maximum possible number of overlaps. Letting $C_k = V_{box}N_a^{(k)}/2N_p$ and $B_2^{hc} = -V_{box}N_o/2N_p$, eq 11 can be rewritten as

$$B_2 = B_2^{hc} - [C_1(e^{\beta\epsilon}-1) + C_2(e^{2\beta\epsilon}-1) + C_3(e^{3\beta\epsilon}-1) + \ldots + C_m(e^{m\beta\epsilon}-1)] \tag{12}$$

The first term on the right-hand side of eq 12 is the contribution to the second virial coefficient from configurations with hard-core repulsions, the second term is the contribution due to configurations with one attractive overlap, the third term is due to configurations with two attractive overalaps, and so on. The average value of the f-function is determined over 20–25 groups of 2×10^6 chain configurations.

To test our program, we compared our results to Yethiraj and Hall's[15] results for square-well dimers with $\lambda = 0.5$. They determined the second virial coefficient for square-well dimers to be

$$B_2/4v_0 = 1.361 - 3.063(\Theta-1) - 1.025(\Theta-1)^2 - 0.205(\Theta-1)^3 - 0.0198(\Theta-1)^4 \tag{13}$$

where $v_0 = \pi\sigma^3/3$ and $\Theta = \exp(\beta\epsilon)$. The method they used to calculate the second virial coefficient is similar to the method used in this work except that new dimers were grown each time a new configuration was desired. In Table 1 the coefficients C_k for dimers from Yethiraj and Hall's work, obtained by writing eq 13 in powers of Θ are compared to the coefficients C_k for dimers with $\lambda = 0.5$ calculated from this work. The coefficients from eq 13 are within the 95% confidence limits of the corresponding C_k's, which gives us confidence that the two methods are equivalent.

Table 2. Hard-Core Contribution to the Second Virial Coefficient of Square-Well Chains

n	B_2^{hc}	chain placements
2	5.703(9)	50×10^6
3	10.31(2)	50×10^6
4	15.84(3)	40×10^6
8	46.0(2)	40×10^6
16	139.0(5)	40×10^6
24	268.5(15)	40×10^6
50	928(7)	40×10^6

3. Second Virial Coefficients for Square-Well Chains

3.1. Monte Carlo Results. Our Monte Carlo results for the coefficients B_2^{hc} and C_1 through C_m for chains of length n = 2, 3, 4, 8, 16, 24, and 50 and well widths λ = 0.25, 0.3, 0.4, 0.5, 0.6, 0.7, 0.75, and 1.0 are listed in Tables 2–9. Table 2 lists B_2^{hc} for chains of length 2, 3, 4, 8, 16, 24, and 50. The result for dimers agrees with the analytic result, $B_2 = 5.701$, of Isihara.[16] Tables 3–9 list values for C_k for n = 2, 3, 4, 8, 16, 24, and 50, respectively. The numbers in parentheses in the tables are the 95% confidence limits, which are determined by calculating subaverages of B_2^{hc} and C_k over every 2 million configurations. The coefficients C_k have more relative uncertainty as k, the number of attractive overlaps, increases. This means that values for B_2 calculated from eq 12 will have more random error as the temperature is decreased, because as the temperature is decreased the configurations with a large number of overlaps are weighted much more heavily than the configurations with fewer overlaps. In Figures 1–3 the second virial coefficients for square-well chains with well widths of λ = 0.25, 0.5, and 0.75, respectively, are plotted as a function of inverse temperature, $1/T^* = \epsilon/kT$. At $1/T^* = 0$, the square-well-chain second virial coefficient reduces to the hard-sphere-chain second virial coefficient. As the temperature is decreased, the second virial coefficient decreases; the temperature at which the second virial coefficient equals zero is the theta temperature. Below the theta temperature the second virial coefficient is negative. The points in Figures 1–3 are Monte Carlo integrations to determine the second virial coefficient; the lines are the closed-form expression for the second virial coefficient of square-well chains which will be presented in section 3.3.

3.2. Theta Temperature Determination. The theta temperature is of interest because at this temperature the attractive and repulsive contributions to the second virial coefficient cancel each other, and the chains exhibit ideal chain behavior. One definition of the "theta temperature", $T_\theta^*(n) = kT_\theta(n)/\epsilon$, is the temperature at which the second virial osmotic virial coefficient, B_2, equals zero. This definition is analogous to the "Boyle temperature" of a real gas. Another common definition of the theta temperature is the temperature at which an isolated polymer chain behaves like a random coil. These two definitions are not necessarily equivalent.[17] Since our goal is to calculate thermodynamic properties at low density, we focus on the first definition, $B_2(T_\theta(n)) = 0$. The dilute solution theory of Flory,[18] which neglects the end effects of the chains, predicts that the theta temperature is independent of chain length. For chains where end effects are important, there is evidence that the theta temperature is a function of chain length. For example, experiments have shown that the theta temperature for star polymers

Table 3. Coefficients C_k in Eq 12 for the Second Virial Coefficient of Dimers

	λ							
k	0.25	0.30	0.40	0.50	0.60	0.70	0.75	1.00
1	3.346(9)	4.002(11)	5.270(11)	6.489(9)	7.639(11)	8.729(14)	9.24(2)	11.74(2)
2	0.559(4)	0.805(5)	1.424(6)	2.22(2)	3.168(6)	4.231(8)	4.797(11)	7.396(12)
3	0.0664(13)	0.112(2)	0.270(2)	0.523(3)	0.874(4)	1.332(6)	1.602(6)	3.660(7)
4	0.0036(3)	0.0078(3)	0.0289(7)	0.0827(11)	0.203(2)	0.427(4)	0.592(4)	2.129(8)

Table 4. Coefficients C_k in Eq 12 for the Second Virial Coefficient of Trimers

	λ							
k	0.25	0.30	0.40	0.50	0.60	0.70	0.75	1.0
1	9.757(20)	10.869(20)	11.392(23)	13.892(24)	4.768(12)	5.605(14)	7.149(18)	8.520(20)
2	1.012(4)	1.411(5)	2.326(8)	3.369(12)	4.470(15)	5.586(18)	6.128(18)	8.412(18)
3	0.1997(21)	0.3255(31)	0.694(4)	1.215(5)	1.864(5)	2.607(6)	3.010(8)	5.086(15)
4	0.0391(8)	0.0733(8)	0.2029(21)	0.4340(32)	0.784(5)	1.252(6)	1.526(6)	3.270(8)
5	0.0068(3)	0.0152(6)	0.0536(10)	0.1432(15)	0.3097(25)	0.582(4)	0.760(5)	2.058(8)
6	0.0006(1)	0.0017(2)	0.0092(5)	0.0343(8)	0.0972(14)	0.2226(26)	0.3178(34)	1.221(6)
7		0.0001(1)	0.0010(2)	0.0057(3)	0.0238(8)	0.0700(15)	0.1101(16)	0.629(4)
8				0.0006(1)	0.0032(2)	0.0136(7)	0.0260(9)	0.2614(30)
9					0.0003(1)	0.0017(2)	0.0034(2)	0.0680(15)

Table 5. Coefficients C_k in Eq 12 for the Second Virial Coefficient of 4-Mers

	λ							
k	0.25	0.30	0.40	0.50	0.60	0.70	0.75	1.00
1	6.238(18)	7.239(22)	9.035(29)	10.58(4)	11.90(4)	13.08(4)	13.63(4)	16.23(4)
2	1.502(12)	2.055(12)	3.267(14)	4.571(26)	5.879(30)	7.111(25)	7.692(27)	10.03(4)
3	0.348(6)	0.556(5)	1.127(8)	1.871(10)	2.737(12)	3.666(16)	4.136(19)	6.322(21)
4	0.0774(21)	0.1462(17)	0.385(5)	0.775(5)	1.314(10)	1.969(10)	2.332(10)	4.333(19)
5	0.0183(9)	0.0386(15)	0.1259(21)	0.306(4)	0.610(4)	1.043(6)	1.308(9)	2.939(9)
6	0.0045(4)	0.0101(7)	0.0402(17)	0.1176(14)	0.2695(30)	0.532(5)	0.704(5)	1.955(10)
7	0.0011(3)	0.0028(3)	0.0125(9)	0.0429(15)	0.1194(27)	0.262(4)	0.370(5)	1.294(7)
8	0.0001(1)	0.0005(2)	0.0033(4)	0.0142(8)	0.0467(11)	0.1241(19)	0.1867(33)	0.841(6)
9			0.0005(1)	0.0036(4)	0.0159(10)	0.0518(19)	0.0855(15)	0.520(7)
10			0.0001(1)	0.0009(2)	0.0050(6)	0.0189(11)	0.0345(18)	0.309(4)
11				0.0001(1)	0.0010(3)	0.0060(5)	0.0116(9)	0.1611(21)
12					0.0002(1)	0.0015(3)	0.0037(5)	0.0767(23)
13					0.0001(1)	0.0004(2)	0.0009(2)	0.0312(14)
14						0.0001(1)	0.0002(1)	0.0109(7)
15								0.0025(3)
16								0.0004(1)

increases as chain length increases.[19,20] Lattice calculations of Janssens and Bellemans[21] and of Dickman[14] for linear chains show that the theta temperature decreases as chain length increases. In this section, we investigate the theta temperature of square-well chains.

We use the Monte Carlo integration results for the second virial coefficient to calculate the theta temperature for square-well chains with $\lambda = 0.25$–1.0. Values for $T_\theta^*(n)$ for square-well chains are listed in Table 10 in units of ϵ/k. The theta temperature was determined from eq 12 by adjusting the temperature until $B_2 = 0$. To estimate the error in the theta temperature, we calculate the theta temperature associated with the values of B_2^{hc} and the C_k's from 20–25 groups of 2 million chain placements and calculate the 95% confidence limits. We find that for $\lambda \leq 0.4$, the theta temperature decreases as chain length increases for $n \geq 3$; for $\lambda \geq 0.6$, the theta temperature increases as chain length increases.

The approach of the theta temperature to its infinite chain value can be described by a scaling relation

$$T_\theta^*(n) - T_\theta^*(\infty) \propto n^{-\phi} \tag{14}$$

as pointed out by Dickman.[12] In Table 11 the scaling exponents, ϕ, and the values for the infinite chain length theta temperature, $T_\theta^*(\infty)$, are listed for square-well chains with $\lambda = 0.6$, 0.7, 0.75, and 1.0; they were determined simultaneously by a least squares fit to a log–log plot of $T_\theta^*(n)-T_\theta^*(\infty)$ versus chain length. The value of $T_\theta^*(\infty)$ was adjusted to find the maximum in the correlation coefficient of the least squares fit. The dependence of the theta temperature on chain length is well described by the scaling relation in eq 14 for $\lambda \geq 0.6$. A fit of the scaling curve to the data for $\lambda = 0.7$ is shown in Figure 4. As the well width decreases, the scaling exponent, ϕ, increases. It appears that at roughly $\lambda = 0.5$ the theta temperature is constant as chain length increases; for smaller well widths the theta temperature decreases as chain length increases, and for larger well widths the theta temperature increases as chain length decreases. We did not attempt to fit the theta temperatures at the smaller well widths to a scaling curve, because the errors in the theta temperature values were relatively large.

The change in the theta temperature with chain length may be understood by considering the effect of increasing chain length on the repulsive and attractive contributions to $B_2(T^*)$. Since the theta temperature is the point at which the repulsive and attractive contributions to $B_2(T^*)$ effectively cancel each other, the change in the theta temperature with chain length depends on the relative sizes of the incremental changes in the attractive and repulsive contributions to $B_2(T^*)$ with increasing chain length. The repulsive contribution to the second virial coefficient is positive, is temperature independent, and increases with chain length. The attractive contribution to the second virial coefficient is negative, is temperature dependent (its absolute value increases with temperature), and becomes more negative as chain length increases. For large λ ($\lambda \geq 0.6$), the incremental decrease in the attractive contribution to $B_2(T^*)$ with increasing n is larger than the

Table 6. Coefficients C_k in Eq 12 for the Second Virial Coefficient of 8-Mers

	λ							
k	0.25	0.30	0.40	0.50	0.6	0.7	0.75	1.0
1	12.69(7)	14.42(8)	17.26(10)	19.40(11)	21.07(14)	22.48(15)	23.05(15)	25.94(17)
2	3.699(34)	4.902(35)	7.34(5)	9.66(8)	11.75(9)	13.51(9)	14.23(9)	17.07(12)
3	1.079(15)	1.643(18)	3.10(4)	4.75(5)	6.42(6)	8.05(8)	8.78(7)	11.49(6)
4	0.312(9)	0.561(13)	1.304(21)	2.367(26)	3.624(29)	4.96(4)	5.64(5)	8.55(8)
5	0.092(5)	0.187(7)	0.556(10)	1.178(19)	2.053(24)	3.110(34)	3.677(34)	6.45(5)
6	0.0248(21)	0.065(4)	0.233(7)	0.590(11)	1.164(17)	1.921(26)	2.368(29)	4.79(5)
7	0.0070(18)	0.0195(23)	0.094(4)	0.285(7)	0.649(14)	1.207(17)	1.546(21)	3.65(4)
8	0.0017(5)	0.0073(13)	0.0369(28)	0.136(4)	0.356(7)	0.732(13)	0.985(22)	2.713(33)
9	0.0009(4)	0.0019(6)	0.0177(25)	0.065(4)	0.202(7)	0.453(10)	0.634(8)	2.050(32)
10	0.0002(2)	0.0007(4)	0.0058(11)	0.0312(26)	0.104(5)	0.278(9)	0.401(9)	1.539(22)
11	0.0002(2)	0.0004(3)	0.0026(8)	0.0143(22)	0.058(4)	0.167(7)	0.255(9)	1.146(16)
12	0.0001(2)	0.0001(2)	0.0012(7)	0.0063(13)	0.0283(27)	0.099(4)	0.162(7)	0.864(11)
13	0.0001(1)	0.0002(2)	0.0005(3)	0.0037(9)	0.0153(19)	0.0560(29)	0.100(4)	0.646(12)
14			0.0003(2)	0.0016(8)	0.0079(13)	0.0342(22)	0.0592(30)	0.467(10)
15			0.0001(2)	0.0007(3)	0.0054(13)	0.0206(26)	0.0385(27)	0.350(8)
16		0.0001(1)	0.0002(2)	0.0004(3)	0.0024(8)	0.0114(17)	0.0237(24)	0.250(7)
17			0.0001(1)	0.0002(2)	0.0011(5)	0.0071(16)	0.0135(20)	0.188(8)
18				0.0001(1)	0.0006(4)	0.0034(8)	0.0069(13)	0.140(5)
19				0.0001(1)	0.0003(2)	0.0017(6)	0.0051(15)	0.097(5)
20				0.0001(1)	0.0002(2)	0.0011(5)	0.0024(8)	0.073(4)
21					0.0001(2)	0.0006(4)	0.0013(4)	0.0517(33)
22					0.0001(2)	0.0003(3)	0.0007(4)	0.0347(24)
23					0.0001(1)	0.0003(3)	0.0005(3)	0.0221(21)
24						0.0003(3)	0.0005(4)	0.0160(22)
25							0.0001(1)	0.0096(14)
26							0.0001(2)	0.0065(11)
27								0.0039(11)
28								0.0031(10)
29								0.0016(6)
30							0.0001(1)	0.0011(3)
31								0.0008(4)
32								0.0005(4)
33								0.0001(2)
35								0.0001(1)
39								0.0001(1)

incremental increase in the repulsive contribution; hence the theta temperature shifts to higher values of ϵ/kT. At $\lambda \simeq 0.5$, the incremental changes in the attractive and repulsive contributions to $B_2(T^*)$ with increasing n appear to cancel, and hence the theta temperature in independent of n. For small values of λ ($\lambda \leq 0.4$), the incremental decrease in the attractive contribution to $B_2(T^*)$ with increasing n is smaller than the incremental increase in the repulsive contribution; hence the theta temperature shifts to lower values of ϵ/kT.

The lattice chain models studied by Janssens and Bellemans and by Dickman predict that the theta temperature decreases with increasing chain length, like the square-well chains with small well widths. This indicates that in the lattice chain models considered, as chain length is increased, the incremental addition to the attractive contribution of the second virial coefficient is not as great as the incremental addition to the repulsive contribution.

3.3. Closed-Form Expression for the Second Virial Coefficient. We have developed a closed-form expression which fits the second virial coefficient data accurately above the theta temperature. This equation compactly expresses eq 12 for square-well chains and requires that only B_2^{hc}, C_1, and $T_\theta^*(n)$ be determined. It is useful to express the second virial coefficient as the sum of the contributions due to repulsive and attractive chain overlaps, $B_2 = B_2^{rep} + B_2^{att}$. The attractive contribution to the second virial coefficient requires the calculation of C_1, C_2, ..., C_m (see eq 12). To express the attractive contribution in a more compact manner, we relate the occurrence of double overlaps to the occurrence of single overlaps by $cC_1 = C_2$. We assume that the occurrence of k overlaps can be related to the occurrence of $k-1$ overlaps by the same coefficient, $cC_{k-1} = C_k$. By applying this relation recursively, we can write B_2^{att} in terms of C_1 and c

$$-B_2^{att} = C_1(e^{\beta\epsilon} - 1) + cC_1(e^{2\beta\epsilon} - 1) + c^2C_1(e^{3\beta\epsilon} - 1) + ... + c^{m-1}C_1(e^{m\beta\epsilon} - 1) \quad (15)$$

Rearrangement gives

$$B_2^{att} = -C_1[e^{\beta\epsilon}(1 + ce^{\beta\epsilon} + c^2e^{2\beta\epsilon} + ... + c^{m-1}e^{(m-1)\beta\epsilon}) + (1 + c + c^2 + ... + c^{m-1})] \quad (16)$$

This geometric series can be approximated as

$$B_2^{att} = -C_1\left[\frac{e^{\beta\epsilon}}{1 - ce^{\beta\epsilon}} - \frac{1}{1 - c}\right] \quad (17)$$

if $c < 1$; it exactly expresses eq 15 if $m - 1 = \infty$. The total second virial coefficient can then be written as

$$B_2 = B_2^{hc} - C_1\left[\frac{e^{\beta\epsilon}}{1 - ce^{\beta\epsilon}} - \frac{1}{1 - c}\right] \quad (18)$$

where B_2^{hc} and C_1 are determined from Monte Carlo integration and the parameter c is set so that $B_2(T_\theta^*) = 0$.

We have determined the values of B_2^{hc}, C_1, and c for $\lambda = 0.25$–0.75 to be used with our closed-form expression, eq 18, in the following manner. The parameter B_2^{hc} is a function of chain length only and can be estimated using eq 2, which was determined by Yethiraj et al.[7] to be very accurate for $n \geq 12$. Alternatively, the scaling relation

$$B_2^{hc} = 1.409n^2(n - 1)^{-0.3469} \quad (19)$$

Table 7. Coefficients C_k in Eq 12 for the Second Virial Coefficient of 16-Mers

	λ							
k	0.25	0.30	0.40	0.50	0.60	0.70	0.75	1.00
1	27.87(27)	31.17(27)	35.88(32)	39.20(28)	41.49(30)	43.06(33)	43.77(28)	46.87(32)
2	9.25(11)	11.88(13)	17.02(15)	21.28(18)	24.76(21)	27.42(26)	28.50(26)	31.94(22)
3	3.11(6)	4.60(6)	8.03(9)	11.69(12)	14.96(15)	17.79(17)	18.96(18)	22.74(20)
4	1.024(27)	1.747(50)	3.88(6)	6.48(9)	9.32(11)	12.00(15)	13.17(13)	17.61(15)
5	0.366(15)	0.690(19)	1.81(5)	3.60(5)	5.75(8)	8.12(8)	9.30(11)	13.96(11)
6	0.117(10)	0.269(13)	0.862(25)	2.00(5)	3.62(5)	5.45(7)	6.49(7)	11.06(14)
7	0.043(7)	0.105(10)	0.444(18)	0.195(28)	2.22(4)	3.75(6)	4.59(7)	8.81(8)
8	0.0120(24)	0.038(6)	0.200(14)	0.623(19)	1.40(4)	2.56(5)	3.22(5)	7.08(8)
9	0.0057(19)	0.0182(34)	0.090(7)	0.337(16)	0.857(26)	1.717(34)	2.250(32)	5.67(10)
10	0.0012(8)	0.0073(23)	0.043(6)	0.192(14)	0.548(21)	1.153(32)	1.597(40)	4.53(6)
11	0.009(8)	0.0020(12)	0.023(5)	0.100(9)	0.328(15)	0.810(26)	1.111(17)	3.62(7)
12		0.0009(9)	0.0118(32)	0.053(7)	0.201(15)	0.531(18)	0.796(27)	2.95(4)
13		0.0002(4)	0.0045(19)	0.038(5)	0.132(10)	0.358(15)	0.557(30)	2.39(6)
14		0.0002(4)	0.0014(10)	0.019(4)	0.077(8)	0.240(15)	0.384(18)	1.862(36)
15		0.0002(4)	0.0016(12)	0.0100(25)	0.043(6)	0.176(9)	0.269(12)	1.492(40)
16			0.0004(5)	0.0050(16)	0.032(4)	0.100(9)	0.194(12)	1.186(34)
17			0.0002(4)	0.0027(17)	0.018(4)	0.075(7)	0.134(10)	0.946(30)
18				0.0011(10)	0.014(4)	0.048(8)	0.090(10)	0.778(27)
19				0.0004(5)	0.0084(33)	0.031(5)	0.064(10)	0.616(24)
20				0.0007(9)	0.0032(17)	0.024(4)	0.045(7)	0.494(16)
21				0.0002(4)	0.0027(17)	0.0168(28)	0.0275(34)	0.391(17)
22				0.0002(4)	0.0014(12)	0.0105(20)	0.021(5)	0.309(17)
23					0.0011(10)	0.0086(29)	0.0134(27)	0.261(10)
24					0.0009(8)	0.0043(13)	0.0116(34)	0.197(13)
25					0.0002(4)	0.0034(15)	0.0062(20)	0.162(10)
26						0.0018(10)	0.0059(22)	0.124(12)
27					0.0002(4)	0.0016(13)	0.0037(18)	0.101(10)
28					0.0002(4)	0.0005(6)	0.0029(15)	0.077(5)
29						0.0012(10)	0.0014(10)	0.058(5)
30						0.0002(4)	0.0012(8)	0.047(6)
31							0.0004(5)	0.035(5)
32							0.0009(8)	0.031(4)
33							0.0004(5)	0.022(4)
34							0.0004(8)	0.0196(26)
35								0.0130(27)
36								0.0127(31)
37								0.0098(25)
38								0.0066(24)
39								0.0050(24)
40						0.0002(4)		0.0050(22)
41								0.0025(13)
42								0.0029(13)
43							0.0002(4)	0.0032(21)
44								0.0014(12)
45								0.0020(15)
46								0.0018(13)
48								0.0005(6)
49								0.0004(5)
51								0.0004(5)
52								0.0005(6)
51								0.0002(4)
55								0.0002(4)
56								0.0002(4)
57								0.0002(4)

can be used; this is more accurate at shorter chain lengths. The second parameter, C_1, is a function of both well width and chain length. We assume that C_1 can be expressed by a scaling relation which is of the same form as the scaling relation for $B_2^{hc}(n)$,

$$C_1 = An^2(n-1)^\gamma \tag{20}$$

where the leading term, A, and the exponent, γ, are functions of the well width λ. We have found that both A and γ are linear functions of the well width in the region λ = 0.25–0.75; a linear least squares fit gives eq 4. The final term, c, can be determined if B_2^{hc}, C_1, and the theta temperature are known. Since the theta temperature is not a strong function of chain length, we determine its dependence on λ by fitting the theta temperature at n = 16 over the well widths λ = 0.25–0.75 and then using this as an estimate for the theta temperature at all chain lengths. The resulting expression is

$$T_\theta^* = 0.5372(\lambda + 1)^{4.3034} \tag{21}$$

The parameter c can then be determined by solving eq 18 at the theta temperature to yield

$$c = (e^{1/T_\theta^*} + 1)/2e^{1/T_\theta^*} - \frac{1}{2}\left[\left(\frac{e^{1/T_\theta^*}+1}{e^{1/T_\theta^*}}\right)^2 - (4/e^{1/T_\theta^*})\left(1 - \frac{e^{1/T_\theta^*}-1}{B_2^{hc}/C_1}\right)\right]^{1/2} \tag{22}$$

Now we have expressions for B_2^{hc}, C_1, and c and can insert these into eq 18 to determine the second virial coefficient for a specific chain length and square-well width.

In Figures 1–3, we compare this closed-form expression to Monte Carlo results for the second virial coefficient at

Table 8. Coefficients C_k in Eq 12 for the Second Virial Coefficient of 24-Mers

	λ							
k	0.25	0.30	0.40	0.50	0.60	0.70	0.75	1.00
1	45.1(7)	50.0(7)	57.0(10)	61.3(8)	64.4(7)	65.8(7)	66.2(8)	69.2(7)
2	15.60(30)	19.9(4)	27.62(34)	34.2(5)	39.2(6)	43.0(8)	44.2(7)	47.9(5)
3	5.52(16)	7.98(23)	13.81(25)	19.33(38)	24.2(5)	28.6(5)	30.2(5)	34.6(6)
4	2.03(14)	3.40(18)	6.80(21)	11.22(28)	15.61(31)	19.42(32)	21.4(4)	27.1(5)
5	0.71(10)	1.40(11)	3.56(20)	6.55(17)	10.06(24)	13.88(27)	15.20(20)	22.34(41)
6	0.26(4)	0.57(7)	1.74(10)	3.90(12)	6.51(17)	9.50(24)	11.20(24)	18.03(25)
7	0.081(26)	0.20(5)	0.90(10)	2.17(15)	4.24(16)	6.78(20)	7.97(22)	14.77(35)
8	0.039(16)	0.110(29)	0.399(57)	1.32(8)	2.78(14)	4.76(19)	6.04(25)	11.74(28)
9	0.003(4)	0.045(17)	0.22(4)	0.73(6)	1.79(10)	3.25(12)	4.29(16)	9.71(24)
10	0.007(6)	0.021(9)	0.130(20)	0.40(5)	1.18(8)	2.42(10)	3.10(11)	7.95(30)
11	0.0014(30)	0.004(5)	0.080(20)	0.256(33)	0.72(8)	1.70(9)	2.31(14)	6.45(25)
12		0.003(4)	0.031(11)	0.148(31)	0.502(45)	1.19(9)	1.71(8)	5.25(18)
13		0.0014(30)	0.013(9)	0.102(23)	0.341(35)	0.79(5)	1.22(10)	4.29(19)
14	0.0014(30)		0.007(6)	0.052(19)	0.204(33)	0.592(55)	0.83(7)	3.60(16)
15		0.0014(30)	0.0014(30)	0.032(12)	0.134(29)	0.42(4)	0.64(8)	2.91(13)
16			0.0014(30)	0.017(8)	0.094(27)	0.28(4)	0.49(6)	2.50(12)
17			0.0014(30)	0.008(9)	0.069(24)	0.196(35)	0.35(5)	1.97(13)
18				0.003(4)	0.039(12)	0.176(30)	0.26(4)	1.66(15)
19			0.0014(30)	0.003(4)	0.020(10)	0.105(28)	0.186(35)	1.43(9)
20				0.003(4)	0.015(9)	0.069(21)	0.129(28)	1.15(10)
21					0.008(9)	0.043(17)	0.105(27)	0.91(9)
22				0.0014(30)	0.006(6)	0.036(17)	0.073(25)	0.74(7)
23					0.004(5)	0.024(13)	0.049(19)	0.631(6)
24					0.004(7)	0.028(14)	0.043(18)	0.52(7)
25					0.003(4)	0.013(8)	0.028(13)	0.48(5)
26						0.011(9)	0.015(7)	0.35(5)
27				0.0014(30)		0.004(7)	0.011(9)	0.31(4)
28					0.0014(30)	0.003(4)	0.021(11)	0.246(33)
29					0.0014(30)	0.003(4)	0.006(6)	0.185(36)
30						0.0014(30)	0.007(10)	0.160(31)
31						0.0014(30)	0.003(4)	0.092(17)
32							0.0014(30)	0.111(29)
33						0.0014(30)	0.007(7)	0.0727(22)
34						0.0014(30)	0.0014(30)	0.070(27)
35					0.0014(30)			0.052(13)
36								0.042(18)
37							0.0014(30)	0.045(18)
38								0.036(12)
39								0.035(17)
40								0.018(13)
41						0.0014(30)		0.013(7)
42								0.014(8)
43								0.008(8)
44								0.020(10)
45								0.011(9)
46								0.014(13)
47							0.0014(30)	0.003(4)
48								0.007(6)
49								0.004(5)
50								0.0014(30)
52								0.006(6)
53								0.0014(30)
55								0.0014(30)
56								0.003(4)
57								0.0014(30)

chain lengths n = 4, 8, 16, 24, and 50 and at well widths λ = 0.25, 0.50, and 0.75, respectively. For chains of length n = 4, 8, and 16, the closed-form expression is accurate in comparison to the Monte Carlo calculations at all of the well widths considered. For n = 24 and 50, the closed-form expression somewhat underestimates the second virial coefficient above the theta temperature; below the theta temperature, the expression is within the 95% confidence limits. For the longer chain lengths, the Monte Carlo results become a tenuous test of the closed-form expression below the theta temperature because they have such large random error.

4. Low-Density Performance of the Generalized Flory–Dimer Equation of State

4.1. Comparison of Second Virial Coefficients to GF-D Theory Predictions. The second virial coefficients for square-well chains calculated here can be used to test the accuracy of the GF-D theory at low density; in this section we compare the second virial coefficients predicted by the theory to values calculated using the Monte Carlo integration technique described above. The GF-D equation of state for square-well chains is a function of the equation of state for square-well monomers and square-well dimers. The compressibility factor from the generalized Flory–dimer equation of state is differentiated to get the second virial coefficient:

$$\lim_{\rho\to 0}\frac{dZ^{chain}}{d\rho} = B_2(n,\lambda,T^*) = \frac{n}{2}(Y_n + 1)B_2(2,\lambda,T^*) - nY_nB_2(1,\lambda,T^*) \quad (23)$$

The second virial coefficient for square-well monomers[23]

Table 9. Coefficients C_k in Eq 12 for the Second Virial Coefficient of 50-Mers

	λ						
k	0.25	0.30	0.40	0.50	0.60	0.70	0.75
1	114.5(15)	125.3(18)	139.8(23)	147.2(22)	150.5(23)	151.7(22)	152.3(23)
2	43.3(11)	53.7(12)	72.0(13)	86.2(16)	95.6(16)	101.5(16)	103.5(16)
3	16.81(41)	24.2(6)	39.0(9)	52.2(9)	63.4(11)	71.6(11)	74.1(17)
4	6.39(29)	10.32(32)	20.6(6)	32.0(8)	42.4(8)	51.4(10)	55.1(10)
5	2.50(13)	4.51(18)	10.86(21)	19.5(5)	29.0(7)	37.6(8)	41.8(9)
6	0.89(6)	1.99(10)	5.90(18)	11.96(27)	19.8(6)	27.5(6)	30.9(7)
7	0.37(5)	0.90(8)	3.30(22)	7.51(28)	13.22(35)	20.2(5)	23.6(5)
8	0.145(28)	0.41(4)	1.60(9)	4.70(21)	8.99(26)	14.7(4)	17.9(4)
9	0.064(24)	0.151(37)	0.91(7)	2.81(14)	6.27(24)	10.8(3)	13.34(30)
10	0.018(9)	0.08(2)	0.47(7)	1.72(12)	4.19(19)	7.97(27)	10.15(31)
11	0.008(6)	0.039(18)	0.27(4)	1.06(8)	2.95(14)	5.81(24)	7.57(26)
12	0.003(4)	0.014(8)	0.127(28)	0.64(6)	1.95(11)	4.37(12)	5.99(26)
13	0.0014(30)	0.008(9)	0.082(15)	0.39(6)	1.38(11)	3.19(15)	4.50(19)
14		0.003(4)	0.048(18)	0.26(4)	0.91(10)	2.36(13)	3.39(14)
15	0.0014(30)	0.003(4)	0.022(8)	0.15(2)	0.62(6)	1.66(12)	2.59(12)
16	0.0014(30)		0.027(13)	0.098(23)	0.44(5)	1.33(11)	2.00(10)
17		0.0014(30)	0.003(4)	0.045(18)	0.23(4)	0.93(7)	1.46(10)
18		0.0014(30)	0.006(7)	0.036(17)	0.200(31)	0.71(8)	1.14(10)
19				0.022(11)	0.147(25)	0.49(5)	0.90(8)
20			0.0014(30)	0.20(1)	0.095(27)	0.34(4)	0.64(8)
21			0.0014(30)	0.011(11)	0.053(14)	0.297(39)	0.47(6)
22				0.008(6)	0.049(17)	0.21(4)	0.37(5)
23			0.0014(30)	0.003(4)	0.031(13)	0.141(26)	0.29(5)
24				0.0014(30)	0.024(14)	0.13(4)	0.253(35)
25					0.020(14)	0.095(27)	0.168(25)
26				0.0014(30)	0.013(13)	0.062(19)	0.136(30)
27					0.010(8)	0.039(13)	0.104(27)
28				0.0014(30)	0.003(4)	0.045(18)	0.077(24)
29					0.004(5)	0.021(11)	0.070(23)
30					0.003(4)	0.025(12)	0.039(18)
31				0.0014(30)	0.0014(30)	0.013(8)	0.031(15)
32					0.0014(30)	0.007(9)	0.034(15)
33						0.006(6)	0.011(7)
34						0.013(11)	0.015(10)
35						0.004(5)	0.008(8)
36					0.0014(30)	0.0014(30)	0.008(6)
37					0.0014(30)		0.003(4)
38						0.0014(30)	0.007(6)
39							0.004(5)
40						0.0014(30)	0.003(4)
41							0.0014(30)
42						0.0014(30)	0.0014(30)
44							0.0014(30)
46						0.0014(30)	0.003(4)
51							0.0014(30)

Table 10. Theta Temperatures for Square-Well Chains

	λ							
n	0.25	0.30	0.40	0.50	0.6	0.7	0.75	1.0
2	1.414(4)	1.686(5)	2.304(5)	3.040(7)	3.915(7)	4.948(9)	5.531(10)	9.217(16)
3	1.422(2)	1.695(3)	2.326(4)	3.089(5)	4.010(7)	5.115(5)	5.744(9)	9.833(14)
4	1.420(5)	1.694(5)	2.326(5)	3.097(6)	4.036(8)	5.168(10)	5.824(11)	10.101(15)
8	1.407(17)	1.689(15)	2.320(10)	3.096(10)	4.054(12)	5.233(15)	5.914(16)	10.460(26)
16	1.389(12)	1.666(14)	2.296(15)	3.086(18)	4.062(27)	5.263(25)	5.95(5)	10.62(4)
24	1.38(3)	1.66(3)	2.31(5)	3.09(7)	4.09(7)	5.28(7)	5.99(7)	10.70(8)
50	1.371(18)	1.651(2)	2.28(3)	3.068(28)	4.06(5)	5.26(6)	5.95(6)	

is $B_2(1,\lambda,T^*) = b_0[1 - ((\lambda + 1)^3 - 1)(e^{\beta\epsilon} - 1)]$, where $b_0 = (2/3)\pi\sigma^3$; the second virial coefficient for square-well dimers with well widths of λ = 0.25, 0.3, 0.4, 0.5, 0.6, 0.7, 0.75, and 1.00 have been determined here by Monte Carlo integration; the C_k's are listed in Table 3. We use these values to calculate the GF-D theory prediction for the second virial coefficient of square-well chains.

In Figures 5–7, the second virial coefficients predicted by the GF-D theory are compared to the second virial coefficients calculated by Monte Carlo integration and the values calculated by eq 18. The second virial coefficient is calculated at well widths λ = 0.25, 0.5, and 0.75 for three temperatures, two above the theta temperature and one below the theta temperature. At λ = 0.25, the GF-D theory overpredicts the second virial coefficient above the theta temperature as chain length increases but is fairly accurate at $T^* = 1.25$, the only temperature studied which is below T_θ^*. At λ = 0.5, the GF-D theory overpredicts the second virial coefficient at $T^* = 5.0$ but underpredicts the second virial coefficient at $T^* = 3.5$ and below the theta temperature at $T^* = 2.5$. Since the errors in the second virial coefficients calculated by Monte Carlo integration are quite large for chains longer than 16-mers at λ = 0.25 and λ = 0.50 below the theta temperature, these points are not plotted on the graphs. At λ = 0.75, again the second virial coefficient is overpredicted at the highest temperature, $T^* = 10.0$, and underpredicted at $T^* = 7.0$ and below the theta temperature at $T^* = 5.0$ by the GF-D theory. The closed-form expression for the second virial coefficient, eq 18, is also compared to Monte Carlo integration in

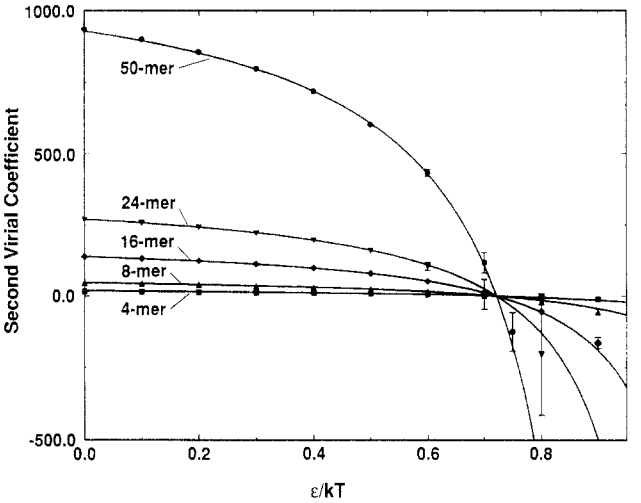

Figure 1. Second virial coefficient for square-well chains of length 4, 8, 16, 24, and 50. For all chains $\lambda = 0.25$. The points are from Monte Carlo integration of eq 6 and the lines are the closed-form expression eq 18. The error bars are the 95% confidence limits.

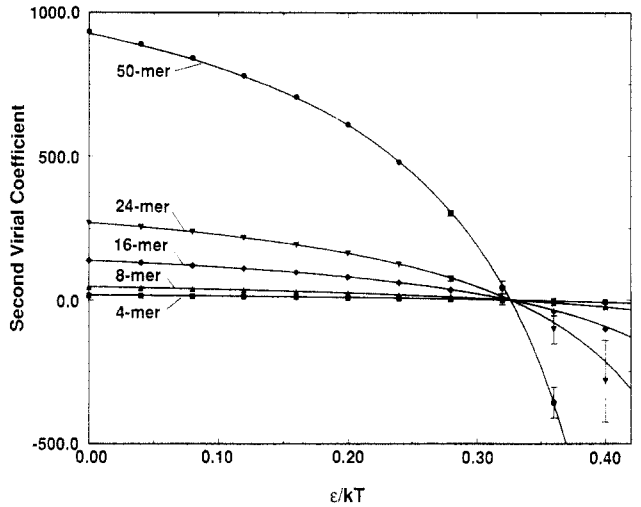

Figure 2. Second virial coefficient for square-well chains of length 4, 8, 16, 24, and 50. For all chains $\lambda = 0.5$. The points are from Monte Carlo integration of eq 6 and the lines are the closed-form expression eq 18. The error bars are the 95% confidence limits.

Figures 5–7. Here we use eq 2 to calculate $B_2^{hc}(n)$, eq 4 to calculate $C_1(n,\lambda)$, and eq 21 to calculate T_θ^*. Above the theta temperature the closed-form expression accurately fits the Monte Carlo data at $\lambda = 0.25$ and 0.5 for $n \geq 4$ and at $\lambda = 0.75$ for $n \geq 8$. Below the theta temperature the closed-form expression fits the Monte Carlo data less accurately than above the theta temperature but is more accurate than the GF-D theory at all of the well widths studied for $n \geq 4$.

4.2. Second Virial Correction to the Generalized Flory–Dimer Equation of State and Truncated Virial Equation of State. The generalized Flory–dimer theory is a mean field theory and is most accurate at high densities, where the compressibility factor of a chain fluid can be approximated in terms of the compressibility factors for monomer and dimer fluids at the same density. At low density, the chain fluid will contain local areas of high site density and local areas of low site density; treating the low density chain fluid as being equivalent to monomer or dimer fluid will lead to an inaccurate estimate of the insertion factor. The inaccurate estimate of the insertion factor at low density is reflected in the second virial coefficient, since higher order terms in the virial expansion

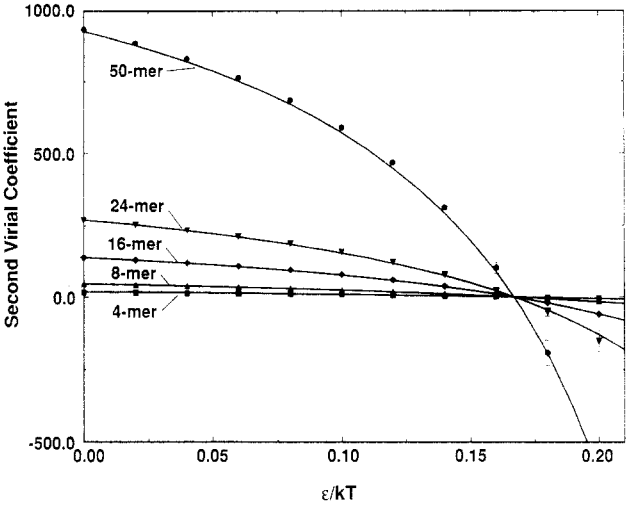

Figure 3. Second virial coefficient for square-well chains of length 4, 8, 16, 24, and 50. For all chains $\lambda = 0.75$. The points are from Monte Carlo integration of eq 6 and the lines are the closed-form expression eq 18. The error bars are the 95% confidence limits.

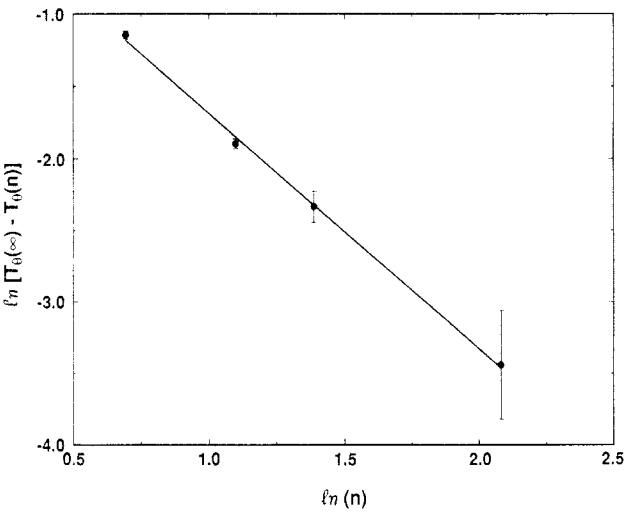

Figure 4. Scaling behavior of square-well chains for $\lambda = 0.7$. The slope of the line is the scaling exponent, $-\phi = -1.75(13)$. The error bars are the 95% confidence limits.

Table 11. Exponent of the Scaling Relation $T_\theta^*(n) - T_\theta^*(\infty) \propto n^{-\phi}$ and Infinite Chain Length Theta Temperatures for Well Widths $\lambda \geq 0.6$

λ	ϕ	$T_\theta(\infty)$
0.60	2.79(6)	4.06
0.70	1.75(13)	5.26
0.75	1.70(3)	5.95
1.0	1.23(3)	10.74

Table 12. Theta Temperatures for Square-Well Chains with Intramolecular Attractions

	λ			
n	0.25	0.50	0.75	1.0
3	1.422(4)	3.093(4)	5.760(9)	9.843(21)
4	1.424(5)	3.109(7)	5.869(15)	10.131(11)
8	1.399(7)	3.101(4)	5.935(10)	10.51(16)
16	1.388(9)	3.066(9)	5.949(8)	10.718(36)

will be negligible at low densities. Yethiraj et al.[7] suggested a virial correction to the GF-D equation of state, explained above, which used their Monte Carlo second virial coefficient calculation results. The second virial coefficients calculated by Monte Carlo integration can also be used in a truncated virial expansion to calculate the compressibility factor of the square-well fluid, although we would

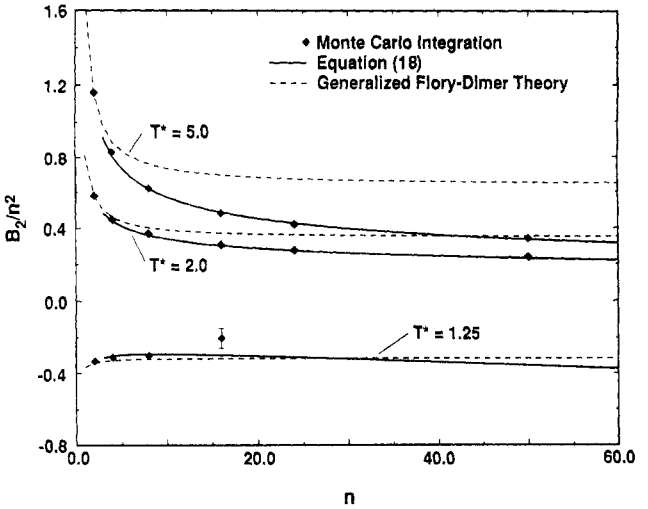

Figure 5. Comparison of the second virial coefficient for square-well chains at $\lambda = 0.25$ predicted by the generalized Flory–dimer theory with Monte Carlo integration and the closed-form expression eq 18.

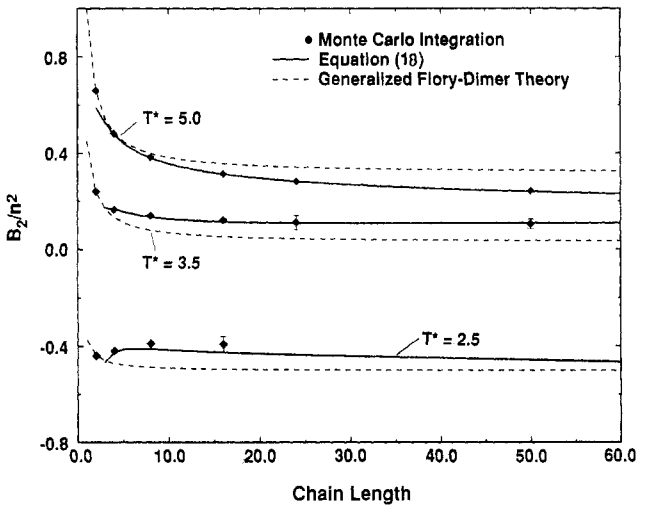

Figure 6. Comparison of the second virial coefficient for square-well chains at $\lambda = 0.5$ predicted by the generalized Flory–dimer theory with Monte Carlo integration and the closed-form expression eq 18.

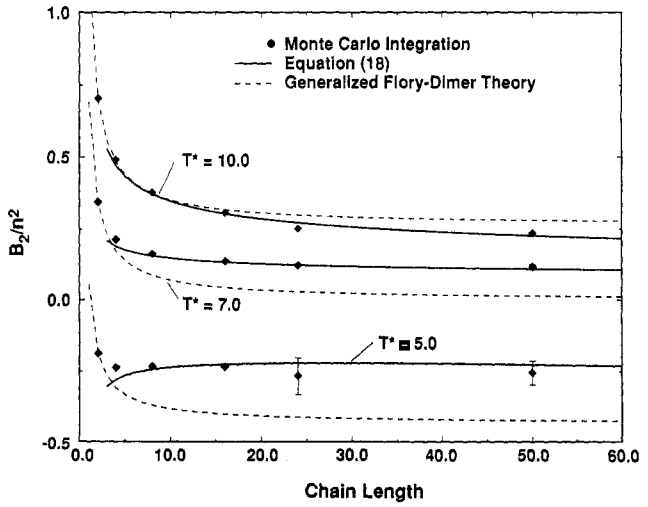

Figure 7. Comparison of the second virial coefficient for square-well chains at $\lambda = 0.75$ predicted by the generalized Flory–dimer theory with Monte Carlo integration and the closed-form expression eq 18.

only expect this equation of state to predict compressibility factors accurately at low density.

Here we compare the compressibility factors predicted by the uncorrected and corrected generalized Flory–dimer equation of state and the truncated virial equation of state, eq 5, to compressibility factors determined from low-density simulations of 8-mers and 20-mers with $\lambda = 0.5$ at $T^* = 10.0$, 5.0, and 3.0. The method we use to calculate the compressibility factor of square-well chains is Monte Carlo simulation in the canonical ensemble, as described by Yethiraj et al.[8] Essentially, square-well chains are put into a box which has hard walls in one dimension and periodic boundaries in the other two dimensions. The chains are moved by the Metropolis algorithm,[9] and the pressure of the system is determined by extrapolating the site density of chain beads to the hard walls. The compressibility factor is given by $Z = n\rho_{wall}/\rho_{bulk}$, where n is the chain length, ρ_{wall} is the site density at the wall, and ρ_{bulk} is the site density in the bulk fluid. In Tables 13 and 14 the results of our low-density simulations are listed. The bulk density, wall density, and compressibility factors are calculated for each state point; between 0.6 million and 2.4 million moves per state point are required to get a precise estimate for the wall density. Equilibration for all of the simulations took less than 0.1 million moves. The simulations were performed on a Cray Y-MP and took ~2 h per million moves for 8-mers and 4 h per million moves for 20-mers.

In Figures 8 and 9 the compressibility factors for 8-mers and 20-mers predicted by the corrected and uncorrected generalized Flory–dimer equation of state are compared to the square-well simulation values. The truncated virial equation of state is also plotted in the low-density insert for 8-mers and up to a density of $\eta = 0.075$ for 20-mers. The generalized Flory–dimer equation of state requires a monomer and dimer equation of state; at $T^* = 10.0$ and 5.0 we use the second-order perturbation theory equations of state of Yethiraj and Hall,[5] and at $T^* = 3.0$ we use the integral equation results of Yethiraj and Hall[10] for dimers and of Smith et al.[11] for monomers. (The perturbation theory gives an analytic equation of state but is not well behaved at low densities and low temperatures.) For both chain lengths and all of the temperatures studied, the corrected equation of state is accurate at very low densities, $\eta < 0.04$. The truncated virial expansion is more accurate than the uncorrected GF-D equation of state but somewhat less accurate than the corrected GF-D equation of state below $\eta = 0.04$. In previous studies of long square-well chains, Yethiraj and Hall[5] and Hall et al.[22] found that the uncorrected equation of state accurately predicts the compressibility factor of 16-mers and 32-mers at volume fractions above $\eta = 0.1$. For hard chains, the second virial coefficient correction works well even at $\eta = 0.2$ for both chain lengths.[7] However, when interchain attractive interactions are introduced, the second virial coefficient correction improves the generalized Flory–dimer equation of state of only in the very low density regime.

5. Effect of Intramolecular Attractions on the Theta Temperature

Many models of chain molecules include attractive interactions between nonneighboring sites on the same chain. For instance, the lattice models of Bellemans and Janssens and of Dickman cited previously include attractive interactions between beads on the same chain. Including attractive interactions will cause an isolated chain to collapse in on itself as the temperature is reduced, causing a decrease in the end-to-end distance and radius of gyration. While including intramolecular attractions has a predictable qualitative effect on the geometry of the

Table 13. Low-Density Simulation Results for the Compressibility Factor of Square-Well 8-Mers with λ = 0.5[a]

n	T^*	cell size	N	η_{avg}	η_{bulk}	η_{wall}	Z
8	3	20 × 20 × 20	29	0.0152	0.0172(4)	0.00221(13)	1.03(6)
8	3	10 × 15 × 15	14	0.0261	0.0335(5)	0.00436(25)	1.04(6)
8	3	10 × 15 × 15	27	0.0503	0.0651(8)	0.0086(5)	1.06(6)
8	3	10 × 10 × 10	18	0.0754	0.0962(20)	0.0123(12)	1.02(10)
8	3	10 × 10 × 10	24	0.1005	0.124(1)	0.0183(14)	1.18(9)
8	5	20 × 20 × 20	29	0.0152	0.0169(1)	0.00224(21)	1.06(3)
8	5	10 × 15 × 15	14	0.0261	0.0325(3)	0.00463(16)	1.14(4)
8	5	10 × 15 × 15	27	0.0503	0.0605(3)	0.0103(5)	1.36(6)
8	5	10 × 10 × 10	18	0.0754	0.0830(9)	0.0171(8)	1.65(8)
8	5	10 × 10 × 10	24	0.1005	0.114(2)	0.0288(11)	2.02(8)
8	5	10 × 10 × 10	48	0.2011	0.207(3)	0.119(8)	4.58(32)
8	10	20 × 20 × 20	29	0.0152	0.0169(2)	0.00247(8)	1.17(4)
8	10	10 × 15 × 15	14	0.0261	0.0316(2)	0.00494(32)	1.25(8)
8	10	10 × 15 × 15	27	0.0503	0.0585(7)	0.0118(6)	1.62(8)
8	10	10 × 10 × 10	18	0.101	0.1091(9)	0.0352(16)	2.58(12)
8	10	10 × 10 × 10	24	0.201	0.202(2)	0.149(5)	5.89(20)

[a] The first dimension in the cell size is the distance between hard walls; the other two dimensions have periodic boundaries. Cell dimensions are expressed in terms of a unit hard-core diameter for the chain beads. N is the number of chains in the cell.

Table 14. Low-Density Simulation Results for the Compressibility Factor of Square-Well 20-Mers with λ = 0.5[a]

n	T^*	cell size	N	η_{avg}	η_{bulk}	η_{wall}	Z
20	3	20 × 23 × 23	15	0.0148	0.0200(7)	0.00098(10)	0.98(11)
20	3	20 × 20 × 20	19	0.0249	0.0308(18)	0.00169(25)	1.10(17)
20	3	20 × 20 × 20	38	0.0497	0.0588(45)	0.0038(6)	1.28(22)
20	3	15 × 15 × 15	24	0.0745	0.103(4)	0.0060(12)	1.16(15)
20	5	20 × 23 × 23	15	0.0148	0.0184(2)	0.00106(6)	1.15(6)
20	5	20 × 20 × 20	19	0.0249	0.0303(8)	0.00188(14)	1.24(9)
20	5	20 × 20 × 20	38	0.0497	0.0582(14)	0.00535(35)	1.84(13)
20	5	15 × 15 × 15	24	0.0745	0.0875(21)	0.0108(9)	2.47(22)
20	10	20 × 23 × 23	15	0.0148	0.0184(1)	0.00116(6)	1.26(7)
20	10	20 × 20 × 20	19	0.0249	0.0295(3)	0.00221(13)	1.50(9)
20	10	15 × 15 × 15	16	0.0497	0.0592(9)	0.0070(4)	2.37(13)
20	10	15 × 15 × 15	24	0.0745	0.0835(18)	0.0142(8)	3.41(20)

[a] The first dimension in the cell size is the distance between hard walls; the other two dimensions have periodic boundaries. Cell dimensions are expressed in terms of a unit hard-core diameter for the chain beads. N is the number of chains in the cell.

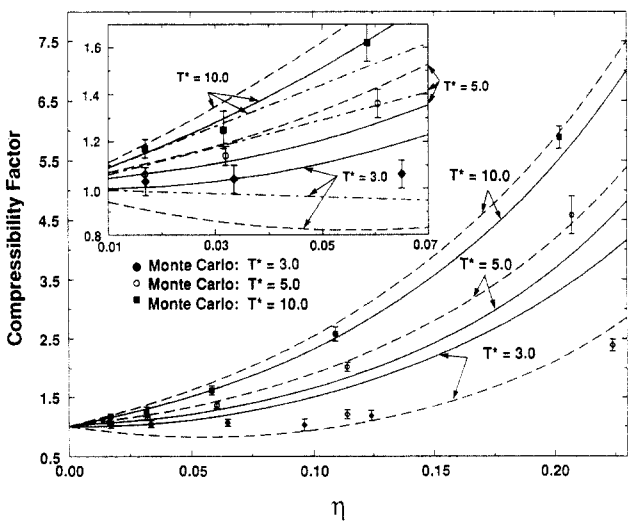

Figure 8. Comparison of low-density compressibility factors for square-well 8-mers calculated by simulation (points) to compressibility factors predicted by the generalized Flory–dimer theory with the second virial coefficient correction (—), without the second virial coefficient correction (– – –), and the truncated virial expansion (– - –) (inset). The unfilled diamonds are results of Yethiraj and Hall.[8]

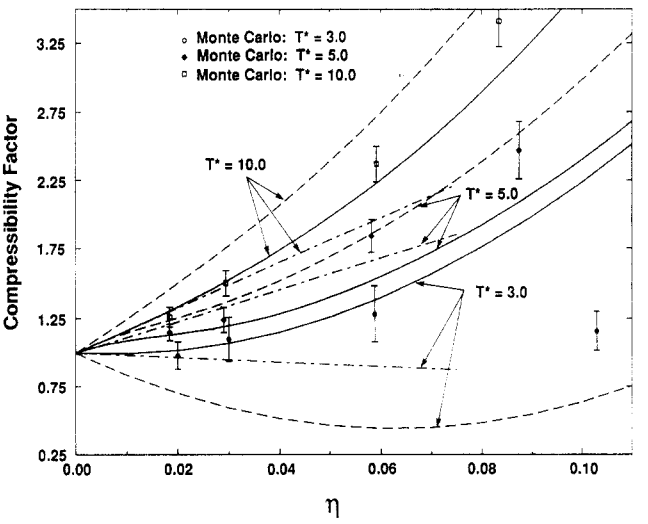

Figure 9. Comparison of low-density compressibility factors for square-well 20-mers calculated by simulation (points) to compressibility factors predicted by the generalized Flory–dimer theory with the second virial coefficient correction (—), without the second virial coefficient correction (– – –), and the truncated virial expansion (– - –).

chain, the effect on the second virial coefficient of the square-well chain is not as obvious. Here we determine the effect of including attractive interactions on the theta temperature behavior of square-well chains. The model we use is the square-well chain considered in the previous section, except that now nonbonded sites on the same chain interact via the square-well potential.

The calculation of the second virial coefficient is more complex when intramolecular attractions are added to the model. If sites on the same chain interact via the hard-sphere potential, the probability of interchain overlaps does not change as the temperature is changed. However, if sites on the same chain interact via the square-well potential, the probability of interachain overlaps does change as the temperature is changed. More specifically, C_k is not a function of temperature for hard-sphere intrachain interactions but is a function of temperature for square-well intrachain interactions.

We describe here the method we use to calculate the second virial coefficient of square-well chains with intramolecular attractions. For a chain which interacts with itself via a square-well potential, initial single-chain configurations are generated starting with a hard-sphere chain, adding the intramolecular attractive potential, and moving the chain until it is relaxed. The "jiggle" move of the translate and jiggle algorithm is used to relax the isolated chain. We move the chain over several sets of jiggle moves, until the radius of gyration and internal energy oscillate about a mean value. At a low temperature (e.g., $T^* = 2.0$ at $\lambda = 0.5$) relaxation occurs after a few thousand moves for an 8-mer and a few hundred thousand moves for a 50-mer. At high temperature (e.g., $T^* > 3.0$ at $\lambda = 0.5$) the chains oscillate about their equilibrium value immediately. Pairs of the resulting relaxed isolated chains are then placed independently in a box and used as initial configurations.

The calculation of the second virial coefficient for chains with intramolecular attractions is essentially the same as for chains without intramolecular attractions, except that we also keep track of the number of interchain overlaps as a function of intrachain overlaps. The C_k's of eq 11 now become functions of temperature. We define $C_k^{(j)}(T^*) = V_{box}N_a^{(k(j))}/2N_p^{(j)}$, where $N_p^{(j)}$ is the number of chain pair placements with j intramolecular attractive overlaps and $N_a^{(k(j))}$ is the number of chain pair placements which have k interchain attractive overlaps, j intrachain attractive overlaps, and no repulsive overlaps. For instance, $C_4^{(2)}$ is proportional to the fraction of chain pair placements with 2 intramolecular overlaps which have 4 intermolecular attractive overlaps. Since any mechanical property can be written as the ensemble average of the property over the various energy levels[23] and since the different energy levels correspond to different numbers of intramolecular attractive overlaps,

$$C_k(T^*) = \frac{\sum_j C_k^{(j)} a_j e^{-j\beta\epsilon}}{\sum_j a_j e^{-j\beta\epsilon}} \tag{24}$$

where a_j is the fraction of chain pairs placed in the box which have j intrachain attractive overlaps at infinite temperature. The following procedure is used to calculate $C_k(T^*)$. We first perform the Monte Carlo integration at one temperature, T^*_{MC}, to evaluate the fraction of chain pairs with j intramolecular overlaps, $f_j(T^*_{MC})$, and the value of $C_k^{(j)}$ for each number of intramolecular overlaps. The summation, $C_k(T^*_{MC}) = \sum_j C_k^{(j)} f_j(T^*_{MC})$, is then calculated. To calculate $C_k(T^*)$ at another temperature, we need to determine the values of a_j. The fraction of configurations with j intramolecular overlaps can be written

$$f_j(T^*_{MC}) = \frac{a_j e^{-j/T^*_{MC}}}{\sum_j a_j e^{-j/T^*_{MC}}} \tag{25}$$

If we know all of the f_i's at T^*_{MC}, then

$$a_j = \frac{f_j(T^*_{MC})/e^{-j/T^*_{MC}}}{\sum_j f_j(T^*_{MC})/e^{-j/T^*_{MC}}} \tag{26}$$

The calculation of $B_1^{hc}(T^*)$ is identical to the calculation of the C_k's. We define $B_2^{hc(j)}$ as the repulsive second virial coefficient for chains with j intramolecular attractive overlaps. Once we know the $B_2^{hc(j)}$'s we can calculate $B_2^{hc}(T^*)$ by eq 24 where we substitute $B_2^{hc}(T^*)$ for $C_k(T^*)$ and $B_2^{hc(j)}$ for $C_k^{(j)}$. Once we know the a_j's, we can calculate $C_k(T^*)$'s and $B_2^{hc}(T^*)$ at any temperature by eq 24 and hence the second virial coefficient by equation 12.

The theta temperature for square-well chains with intramolecular attractions at lengths $n = 3$, 4, 8, and 16 and well widths $\lambda = 0.25$, 0.5, 0.75, and 1.0 has been calculated by Monte Carlo integration. Equation 12 is used to determine the second virial coefficient, and the theta temperature is then determined by adjusting the temperature until $B_2 = 0$. The $C_k^{(j)}(T^*)$'s are calculated for 10 groups of 2 million chain per placements, giving 10 theta temperature estimates; we average the theta temperature and perform an error analysis using these 10 estimates. In Table 12, the theta temperatures for each well width and chain length are listed. For the smallest well width, $\lambda = 0.25$, the theta temperature decreases as chain length increases; for the large well widths, $\lambda = 0.75$ and $\lambda = 1.00$, the theta temperature increases as chain length increases. Thus we conclude that, for all of the chain lengths considered, inclusion of intramolecular attractions has little effect on the theta temperature; all of the theta temperatures for chains with intramolecular attractions are within 1% of the corresponding theta temperature for square-well chains with hard-sphere intrachain interactions. Similarly, Yethiraj and Hall[5] found that including intrachain interactions has only a small effect on the equation of state and the compressibility factor of square-well chains of length $n = 8$ and 16 near the theta temperature ($T^* = 3.0$). At sufficiently low temperatures, however, intramolecular attractions should have a much greater impact, resulting in chain collapse and a significant difference between second virial coefficients for chains with and without intramolecular attractions. We did not study collapsed chains in this paper because our Monte Carlo method is not precise enough for chains of length $n \geq 16$ below the theta temperature.

6. Conclusion

In this paper we have calculated the second virial coefficient of square-well chains with chain lengths $n =$ 2–50 and well widths ranging from $\lambda = 0.25$ to $\lambda = 1.0$. A closed-form expression for the second virial coefficient was presented which is a function of the hard-sphere second virial coefficient, $B_2^{hc}(T^*)$, the attractive portion of the second virial coefficient due to single intrachain attractive overlaps, C_1, and the theta temperature of the square-well chain, T_θ. The approximate expression accurately fits the data calculated by Monte Carlo integration for chains of length $n = 4$–50 and well widths $\lambda = 0.25$–0.75. The theta temperature is constant as chain length increases for $\lambda = 0.5$, decreases as chain length increases for $\lambda > 0.5$, and increases as chain length increases for $\lambda > 0.5$. For $\lambda \geq 0.6$, the departure of the theta temperature from its infinite chain length value is accurately described by a scaling law. Including intrachain interactions has little effect on the theta temperature of square-well chains; adding intramolecular attractions to square-well chains of length $n \leq 16$ changed the theta temperature by <1%.

The low-density performance of the generalized Flory–dimer theory was tested in two ways, first, by comparing the second virial coefficients predicted by the theory to our Monte Carlo results, and second, by comparing compressibility factors determined by simulation. For all of the well widths studied, the GF-D theory overpredicts

the second virial coefficient at high temperatures, as was found in the infinite temperature limit (hard chains) by Yethiraj and Hall.[7] Near the theta temperature, the GF-D theory underpredicts the second virial coefficient for λ = 0.5 and 0.75, while at λ = 0.25 the theory agrees well with the Monte Carlo data just below the theta temperature, at T^* = 1.25. The modification to the GF-D equation of state proposed by Yethiraj and Hall for hard chains was extended to square-well chains and tested against simulation. The modified equation of state predicts compressibility factors very accurately in the very low density regime ($\eta < 0.04$), and somewhat more accurately than the second virial prediction for the compressibility factor at very low densities, but fails to improve the equation of state at higher densities.

Acknowledgment. This work was supported by the Director, Office of Energy Research, Office of Basic Sciences, Chemical Sciences Division of the U.S. Department of Energy under Contract No. DE-FG05-91ER14181. Acknowledgement is made to the donors of the Petroleum Research Fund, administered by the American Chemical Society, for partial support of this research. We gratefully acknowledge the North Carolina Supercomputing Center for time on their Cray Y-MP supercomputer.

References and Notes

(1) Thiesen, M. *Ann. Phys.* 1885, *24*, 467.
(2) Kamerlingh Onnes, H. *Commun. Phys. Lab. Leiden* **1901**, Nos. 71 and 74.
(3) Mayer, J. E. *J. Chem. Phys.* **1937**, *5*, 67.
(4) Dickman, R.; Hall, C. K. *J. Chem. Phys.* **1986**, *85*, 4108.
(5) Yethiraj, A.; Hall, C. K. *J. Chem. Phys.* **1986**, *95*, 8494.
(6) Honnell, K. G.; Hall, C. K. *J. Chem. Phys.* **1990**, *90*, 1841.
(7) Yethiraj, A.; Honnell, K. G.; Hall, C. K. *Macromolecules* **1992**, *25*, 3979.
(8) Yethiraj, A.; Hall, C. K. *J. Chem. Phys.* **1991**, *95*, 1999.
(9) Metropolis, N.; Rosenbluth, A. W.; Rosenbluth, M. N.; Teller, A. H.; Teller, E. *J. Chem. Phys.* **1953**, *21*, 1087.
(10) Yethiraj, A.; Hall, C. K. *Mol. Phys.* **1991**, *72*, 691.
(11) Smith, W. R.; Henderson, D.; Tago, Y. *J. Chem. Phys.* **1977**, *67*, 5308.
(12) Dickman, R. *J. Chem. Phys.* **1992**, *96*, 1516.
(13) Yamakawa, H. *Modern Theory of Polymer Solutions*; Harper and Row: New York, 1971.
(14) Dickman, R.; Hall, C. K. *J. Chem. Phys.* **1988**, *89*, 3168.
(15) Yethiraj, A.; Hall, C. K. *Mol. Phys.* **1991**, *72*, 619.
(16) Isihara, A. *J. Chem. Phys.* **1951**, *19*, 397.
(17) Bruns, W. *Macromolecules* **1984**, *17*, 2826.
(18) Flory, P. *Principles of Polymer Chemistry*; Cornell University Press: Ithaca, NY, 1953; pp 496–540.
(19) Bauer, B. J.; Hadjichristidis, N.; Fetters, L. J. *Macromolecules* **1980**, *13*, 102.
(20) Roovers, J. E. L.; Bywater, S. *Macromolecules* **1974**, *7*, 443.
(21) Janssenns, M.; Bellemans, A. *Macromolecules* **1976**, *9*, 303.
(22) Hall, C. K.; Yethiraj, A.; Wichert, J. M. *Fluid Phase Equilib.* **1993**, *83*, 313.
(23) McQuarrie, D. A. *Statistical Mechanics*; Harper and Row: New York, 1976.